

Article

Towards Quantum Noise Squeezing for 2-Micron Light with Tellurite and Chalcogenide Fibers with Large Kerr Nonlinearity

Arseny A. Sorokin ¹, Gerd Leuchs ^{1,2,3} , Joel F. Corney ⁴, Nikolay A. Kalinin ^{1,2}, Elena A. Anashkina ^{1,5,*}  and Alexey V. Andrianov ¹

¹ Institute of Applied Physics of the Russian Academy of Sciences, 46 Ulyanov Street, 603950 Nizhny Novgorod, Russia

² Max Planck Institute for the Science of Light, Staudtstr. 2, D-91058 Erlangen, Germany

³ Department of Physics, Friedrich-Alexander-Universität Erlangen Nürnberg, D-91058 Erlangen, Germany

⁴ School of Mathematics and Physics, The University of Queensland, Brisbane, QLD 4072, Australia

⁵ Advanced School of General and Applied Physics, Lobachevsky State University of Nizhny Novgorod, 23 Gagarin Ave., 603022 Nizhny Novgorod, Russia

* Correspondence: elena.anashkina@ipfran.ru

Abstract: Squeezed light—nonclassical multiphoton states with fluctuations in one of the quadrature field components below the vacuum level—has found applications in quantum light spectroscopy, quantum telecommunications, quantum computing, precision quantum metrology, detecting gravitational waves, and biological measurements. At present, quantum noise squeezing with optical fiber systems operating in the range near 1.5 μm has been mastered relatively well, but there are no fiber sources of nonclassical squeezed light beyond this range. Silica fibers are not suitable for strong noise suppression for 2 μm continuous-wave (CW) light since their losses dramatically deteriorate the squeezed state of required lengths longer than 100 m. We propose the generation multiphoton states of 2-micron 10-W class CW light with squeezed quantum fluctuations stronger than -15 dB in chalcogenide and tellurite soft glass fibers with large Kerr nonlinearities. Using a realistic theoretical model, we numerically study squeezing for 2-micron light in step-index soft glass fibers by taking into account Kerr nonlinearity, distributed losses, and inelastic light scattering processes. Quantum noise squeezing stronger than -20 dB is numerically attained for a customized As_2Se_3 fibers with realistic parameters for the optimal fiber lengths shorter than 1 m. For commercial As_2S_3 and customized tellurite glass fibers, the expected squeezing in the -20 – -15 dB range can be reached for fiber lengths of the order of 1 m.



Citation: Sorokin, A.A.; Leuchs, G.; Corney, J.F.; Kalinin, N.A.; Anashkina, E.A.; Andrianov, A.V. Towards Quantum Noise Squeezing for 2-Micron Light with Tellurite and Chalcogenide Fibers with Large Kerr Nonlinearity. *Mathematics* **2022**, *10*, 3477. <https://doi.org/10.3390/math10193477>

Academic Editor: Dmitry Makarov

Received: 23 August 2022

Accepted: 19 September 2022

Published: 23 September 2022

Publisher's Note: MDPI stays neutral with regard to jurisdictional claims in published maps and institutional affiliations.



Copyright: © 2022 by the authors. Licensee MDPI, Basel, Switzerland. This article is an open access article distributed under the terms and conditions of the Creative Commons Attribution (CC BY) license (<https://creativecommons.org/licenses/by/4.0/>).

1. Introduction

The branch of quantum optics operating with light states with macroscopic amplitudes and field intensities and well-defined nonclassical properties at the same time has recently attracted much attention. In particular, it is of great interest to study the generation and transportation of bright squeezed light, which refers to nonclassical multiphoton states with fluctuations in one of the quadrature field components below the vacuum level [1]. Squeezed light has found applications in quantum light spectroscopy, quantum telecommunications, including quantum key distribution, quantum computing with continuous variables, quantum memory, and precision quantum metrology with accuracy above the standard quantum limit [2–8] as well as in such ultrasensitive measurements as detecting gravitational waves [9–11]. It has been shown that bright squeezed light sources can be used to demonstrate the effect of quantum teleportation [12]. Additionally, higher-order

spatial-mode squeezed light can be used for biological particle tracking measurements [13]. The possibilities of employing higher-order Hermite–Gaussian modes to form squeezed light have been discussed [14–16].

Many technologies for generating squeezed light have been developed over the last few decades. However, there has been a revival of interest in novel optimized squeezing schemes based on Kerr nonlinearity driven by advances in waveguide fabrication technologies and by prospective applications. The development of new highly nonlinear materials and technologies for producing low-loss fibers and the growing demand for squeezed light in an extended wavelength range encourage the performance of in-depth theoretical analyses. Nonclassical squeezed light can be best obtained from light with a level of field quadrature fluctuations that is already close to the quantum limit by propagating it through a nonlinear medium such as an optical parametric system, an optical fiber with Kerr nonlinearity, or an atomic ensemble [1].

Different nonlinear processes lead to the generation of different types of squeezed light with notable difference in their properties. Nonlinear media with quadratic nonlinearity are widely used to produce squeezed vacuum states in the process of parametric down-conversion. Vacuum-squeezed states have zero mean amplitude and a nonzero mean photon number. By now, this method has achieved record squeezing values [17] and has found many applications. However, there are certain limitations associated with this method. Low-loss crystals with high quadratic nonlinearity are required, and special arrangements are needed to fulfill the phase-matching conditions between the pump and the generated squeezed light. The detection scheme requires either photon-resolving detectors or the use of a local oscillator phase-locked to the squeezed light. Moreover, the wavelength of the generated squeezed light is far from the pump wavelength, requiring some additional wavelength conversion stages when using commonly available laser sources to produce squeezed light in the desired wavelength range.

A simpler and broadband squeezing setup can be constructed using the non-resonant Kerr nonlinearity, which can be especially efficient in optical fibers offering a long interaction distance. Fiber-based setups generate squeezed light with a large mean amplitude in the vicinity of the pump wavelength. The use of polarization-maintaining fibers and employing the polarization squeezing technique helps to make the generation and detection schemes robust [18].

Squeezed light can also be generated in atomic ensembles. However, the level of directly observed squeezing (~ 3.5 dB)—relevant for applications—that has been achieved in experiments so far is moderate when compared to other generation methods [19].

Nonclassical light has an important advantage in terms of applications in quantum telecommunications if it is directly compatible with fiber optics. At present, quantum noise squeezing in silica optical fibers at a wavelength of about $1.55\text{ }\mu\text{m}$ has been experimentally achieved in a number of studies [18,20–25]. The record value for experimentally attained squeezing in optical fibers is -6.8 dB (-10.4 dB when correcting for linear losses) [25].

One of the challenges of quantum optics is the extension of the available wavelength range of nonclassical light sources, which is important for many applications. For instance, next-generation gravitational wave detectors are likely to operate at a wavelength of $2\text{ }\mu\text{m}$, but they require noise suppression stronger than -10 dB relative to the shot-noise level [10]. Similar arguments apply to other high-precision measuring devices. Two-micron fiber lasers with a noise level close to the quantum limit are being actively developed [26,27], and the further suppression of the quantum fluctuations of these sources in all-fiber systems is of great practical interest. At present, from the point of view of quantum fiber optics, the range around $1.5\text{ }\mu\text{m}$ has been mastered, but there are no fiber sources of nonclassical light beyond this range, although silica fiber sources of classical light in the $1\text{--}2\text{ }\mu\text{m}$ range are diversified and are very widespread [28–31]. In standard silica fibers with a relatively low Kerr nonlinear coefficient ($\sim 1\text{ (W km)}^{-1}$), losses grow significantly as the wavelength increases (from 0.2 dB/km at $1.55\text{ }\mu\text{m}$ to $20\text{--}50\text{ dB/km}$ at $2\text{ }\mu\text{m}$), which makes them unsuitable for quantum applications. Note that optical losses are one of the most important

factors limiting quantum effects in optical fibers (which is discussed and explained in detail in [32]). However, there are special non-silica soft glasses with giant nonlinearity [33] that have comparable loss coefficients but that can generate nonclassical states of light with a significant reduction in the required length. Examples of such fibers include chalcogenide and tellurite fibers with strong localization of the field inside a small core. Non-oxide chalcogenide glasses consist of one or more chalcogens: S, Se, or Te, in combination with elements such as As, Ge, Sb, P, In, Ga, etc. [33]. Tellurite glasses are based on tellurium dioxide [33]. The nonlinear Kerr coefficients of these soft glass fibers can be 2–4 orders of magnitude higher than the nonlinear coefficients of standard silica fibers [34–40], so the required fiber length can be reduced significantly, and the influence of loss can be mitigated. Note that optical losses as low as 20 dB/km for tellurite fibers [41], 12 dB/km for As_2S_3 fibers [42], and 60 dB/km for As_2Se_3 fibers [43] have been reported. Moreover, theoretical estimates show that losses in chalcogenide fibers can be significantly reduced (down to 0.5 dB/km) by increasing the material purity [44]. The use of such fibers in classical nonlinear optics experiments is well established, but their potential for quantum applications, such as in generating nonclassical multiphoton states of light, has hardly been investigated as of yet.

To design new experiments, we revisit theoretical models and prospective experimental arrangements with reasonable realistic parameters using numerical modeling.

Recently, using chalcogenide glass fibers to squeeze continuous-wave (CW) light at a wavelength of 2 μm was proposed, and very simple analytical estimates confirmed the promise of this approach [45]. The model only took into account the action of the Kerr nonlinearity, losses were assumed to be lumped at the output end of the fiber, and other processes were neglected [45]. In this paper, we numerically study squeezing for 2-micron light in chalcogenide and tellurite step-index fibers using a more realistic theoretical model and by taking into account the Kerr nonlinearity, distributed losses, and inelastic light scattering processes. We considered two types of relatively widespread chalcogenide glass fibers (As_2S_3 and As_2Se_3 [46]) and a tellurite glass fiber ($\text{TeO}_2\text{--Bi}_2\text{O}_3\text{--ZnO--Na}_2\text{O}$) with realistic characteristics as well as a standard telecommunication silica fiber for comparison. We calculate the most important parameters for squeezing in customized As_2Se_3 and tellurite glass fibers and in commercially available As_2S_3 and silica fibers. The problem of calculating the characteristics of a fiber is a classical problem. Its description is based on Maxwell's equations [47]. From the solution of the characteristic equation, eigenvalues are obtained, and these make it possible to calculate effective mode areas and hence nonlinear Kerr coefficients as well as the group velocity dispersion [47]. Next, we perform detailed numerical studies and identify the factors that limit quantum noise squeezing by taking into account realistic fiber parameters. It is not a trivial task to simulate such a complex system with allowance for real nonlinear response functions, including the instantaneous Kerr and the delayed Raman contributions, which differ significantly for different glasses. Here, we use an advanced numerical simulation method based on the construction of a set of solutions of the stochastic nonlinear Raman-modified Schrödinger equation in phase space, which is equivalent with an appropriate choice of simulation parameters to the solution of the Fokker–Planck equation for the Wigner distribution of the state of a quantum system. We compare the squeezing efficiency for 2 μm CW light in different fibers and reveal the limiting factors. We assume that the system operates at room temperature rather than at a cryogenic temperature. The possibilities of quantum noise suppression in soft glass fibers were compared with the modeling results of the same effect in a standard silica fiber.

2. Methods

To calculate the step-index parameters of the As_2Se_3 , As_2S_3 , tellurite, and silica fibers we use a well-known approach based on numerically solving Maxwell's equations for axially symmetric geometry [47]. An electric field $\mathbf{E}(t, x, y, z)$ of the light wave (where t is

time, and x, y, z are the Cartesian coordinates) with almost linear polarization along the x -axis propagating in an optical fiber along the z -axis can be presented in the form [47]:

$$E(t, x, y, z) = \frac{1}{2} \hat{x} \left[F(x, y) A(t, z) e^{i\beta_0 z} e^{-i\omega_0 t} + c.c. \right] \quad (1)$$

where $A(t, z)$ is a complex and slowly varying envelope; the function $F(x, y)$ characterizes the transverse mode structure of the fiber; ω_0 is the central angular frequency ($\omega_0 = 2\pi f_0 = 2\pi c/\lambda_p$, c is the speed of light, and λ_p is the central (pump) wavelength); $\beta_j = (d^j \beta / d\omega^j)_{\omega=\omega_0}$; β is a propagation constant; and ω is the angular frequency detuning from ω_0 .

For an axially symmetric fiber, $F(x, y) = F(r) e^{il\varphi}$, $l = 0, 1, 2, \dots$, and r and φ are polar coordinates. The equation determining $F(r)$ is obtained from Maxwell's equations. The solution is well known for the case of a step-index fiber with a core radius of $a = d/2$ (d is the diameter of the fiber core) [47]:

$$F(r) = \begin{cases} J_l(kr), & r \leq a \\ C_{clad} K_l(qr), & r \geq a \end{cases} \quad (2)$$

where J_l is a Bessel function, and K_l is a modified Bessel function.

$$\kappa = \sqrt{n_{core}^2 k_0^2 - \beta^2}, \quad q = \sqrt{\beta^2 - n_{clad}^2 k_0^2}, \quad (3)$$

n_{core} and n_{clad} are frequency-dependent refractive indices of the core and cladding, respectively; $k_0 = \omega_0/c$; and the constant C_{clad} is determined according to the boundary condition $J_l(\kappa a) = C_{clad} K_l(qa)$. The propagation constant β is found from the characteristic equation [47]:

$$\left[\frac{J'_l(U)}{U J_l(U)} + \frac{K'_l(W)}{W K_l(W)} \right] \left[\frac{J'_l(U)}{U J_l(U)} + \frac{n_{clad}^2}{n_{core}^2} \frac{K'_l(W)}{W K_l(W)} \right] = l^2 \left(\frac{1}{U^2} + \frac{1}{W^2} \right) \left(\frac{1}{U^2} + \frac{n_{clad}^2}{n_{core}^2} \frac{1}{W^2} \right), \quad (4)$$

where $U = \kappa a$, and $W = qa$. To numerically solve Equation (4), we used an optimal fourth-order Newton-like method [48].

Frequency-dependent refractive indices were calculated using Sellmeier equations for As_2Se_3 [49], As_2S_3 [49], tellurite [50], and silica [47] glasses. Numerical apertures were calculated as

$$NA = \sqrt{n_{core}^2 - n_{clad}^2}, \quad (5)$$

We considered the fundamental mode to be $l = 0$ and $m = 1$, where m is the solution of Equation (4) in the order of decreasing β . After finding β and $F(r)$, we calculated the second-order dispersion coefficient β_2 and the nonlinear Kerr coefficient γ [47]:

$$\gamma = \frac{4\pi^2 \bar{n}_2 \left[\int_{-\infty}^{\infty} |F(r)|^2 dr \right]^2}{\lambda_p \int_{-\infty}^{\infty} |F(r)|^4 dr}, \quad (6)$$

where \bar{n}_2 is the nonlinear refractive index.

Next, we constructed a set of solutions for the complex amplitude $A(t, z)$ of a CW light field that obeyed the stochastic nonlinear Raman-modified Schrödinger equation [51–54]:

$$\frac{\partial}{\partial z} A(t, z) = i \frac{\beta_2}{2} \frac{\partial^2}{\partial t^2} A(t, z) + \left[i\gamma \int_0^{\infty} dt' R(t - t') |A(t', z)|^2 + i\Gamma^R(t, z) \right] A(t, z) - \frac{\alpha}{2} A(t, z) + \Gamma(t, z), \quad (7)$$

where γ is the nonlinear Kerr coefficient; α is the linear optical losses; $R(t) = (1 - f_R)\delta(t) + f_R \cdot R_R(t)$ is the deterministic nonlinear response function taking into account the instantaneous Kerr response as well as the delayed Raman response $R_R(t)$ with a fractional contribution f_R (Figure 1 shows the spectra of Raman functions $\tilde{R}_R = \frac{1}{\sqrt{2\pi}} \int_{-\infty}^{\infty} R_R(t) e^{i\omega t} dt$

for As_2Se_3 [55], As_2S_3 [56], tellurite [57], and silica [52] glasses); and Γ^R and Γ are the zero-mean delta-correlated model functions describing Raman noise and linear quantum noise, respectively,

$$\Gamma^R(\omega, z) = \frac{1}{\sqrt{2\pi}} \int_{-\infty}^{\infty} \Gamma^R(t, z) e^{i\omega t} dt, \quad (8)$$

$$\Gamma(\omega, z) = \frac{1}{\sqrt{2\pi}} \int_{-\infty}^{\infty} \Gamma(t, z) e^{i\omega t} dt, \quad (9)$$

$$\langle \Gamma^R(\omega, z) \Gamma^{R*}(\omega', z') \rangle = \gamma \hbar \omega_0 \alpha^R(\omega - \omega_0) \left(\frac{1}{2} + \frac{1}{\exp\left(\frac{\hbar|\omega - \omega_0|}{kT}\right) - 1} \right) \delta(\omega - \omega') \delta(z - z'), \quad (10)$$

$$\alpha^R(\omega) = 2 \left| \text{Im} \left(\int_0^{\infty} R(t) e^{i\omega t} dt \right) \right|, \quad (11)$$

$$\langle \Gamma(\omega, z) \Gamma^*(\omega', z') \rangle = \frac{\alpha}{2} \hbar \omega_0 \delta(\omega - \omega') \delta(z - z'), \quad (12)$$

where \hbar is the Planck constant; k is the Boltzmann constant; T is the absolute temperature; f_0 is the central frequency; and ω_0 is the central angular frequency ($\omega_0 = 2\pi f_0 = 2\pi c/\lambda_p$, where c is the speed of light, and λ_p is the pump wavelength).

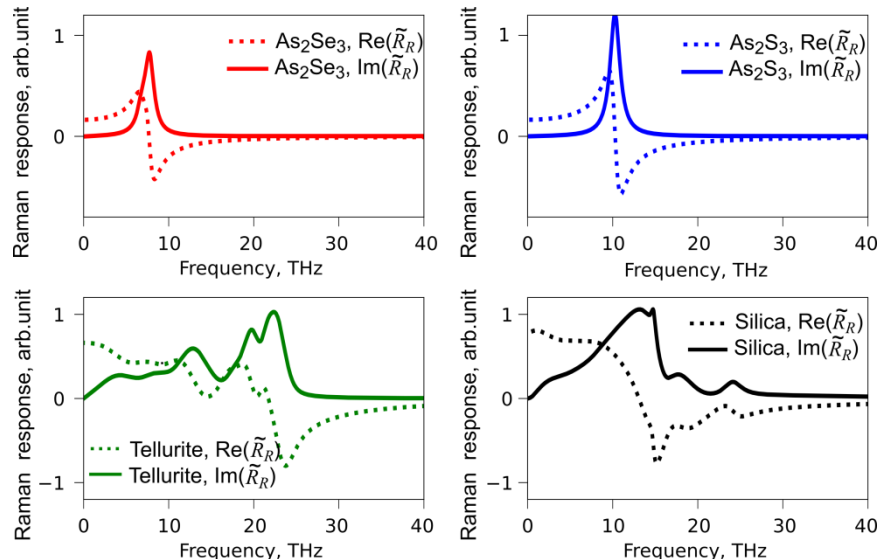


Figure 1. Real and imaginary parts of model Raman response functions in the frequency domain.

The initial complex field amplitude is set as the square root of the pump power P , adding normally distributed delta-correlated stochastic noise $\delta E(0, t)$

$$E(t, 0) = \sqrt{P} + \delta E(t, 0), \quad (13)$$

$$\langle \delta E(t, 0) \delta E^*(t', 0) \rangle = \frac{\hbar \omega_0}{2} \delta(t - t'). \quad (14)$$

We numerically simulated the signal evolution described by Equation (7) using a specially written home-made software. This software is based on the split-step Fourier method and uses fast Fourier transform [47]. We considered a set of 10^3 independent realizations of the initial conditions given by Equations (13) and (14). We assumed that the input signal was a standard quantum-limited one. It has a central symmetric distribution in phase space (Figure 2a shows an example). The evolution of each realization for a certain fiber length shifts the point in phase space [1]. X_1 and X_2 are the two conjugate

quadratures of the electromagnetic field for the considered single-mode (with their mean values subtracted). In Kerr squeezing, the resulting state is neither an amplitude nor a phase-squeezed state. Instead, the state is squeezed for a quadrature that is rotated in phase space by a skewed angle with respect to the direction of the mean field value (we assume without loss of generality that the mean field value lies along the X_1 quadrature). The distribution takes the form of a rotated ellipse-like cloud with uncertainty along the minor axis directions below the standard quantum limit (Figure 2b) [1]. This uncertainty characterizes quantum noise squeezing [1]. We found the minor axis for each cloud corresponding to a certain fiber length (using a modified binary search minimizing the variance along an axis) and calculated the noise suppression relative to the initial noise. Note that losses and inelastic scattering processes deteriorate the degree of squeezing. We neglect guided acoustic wave Brillouin scattering since—as will be shown—the optimal lengths of soft glass fibers are relatively short.

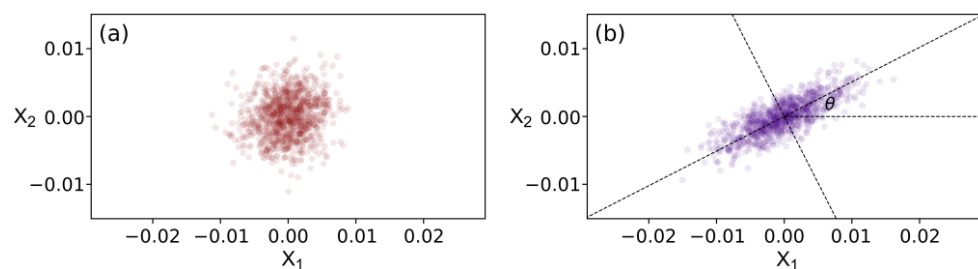


Figure 2. Clouds in single-mode phase space corresponding to coherent-state noise (a) and the squeezed quantum noise (b). X_1 and X_2 are two conjugate quadratures of the electromagnetic field (with their mean values subtracted) of the considered single mode. Each point in the cloud corresponds to a particular realization of the quantum trajectory in the phase space obtained by the modeling; the scattering of the points around the mean values represents the quantum uncertainty.

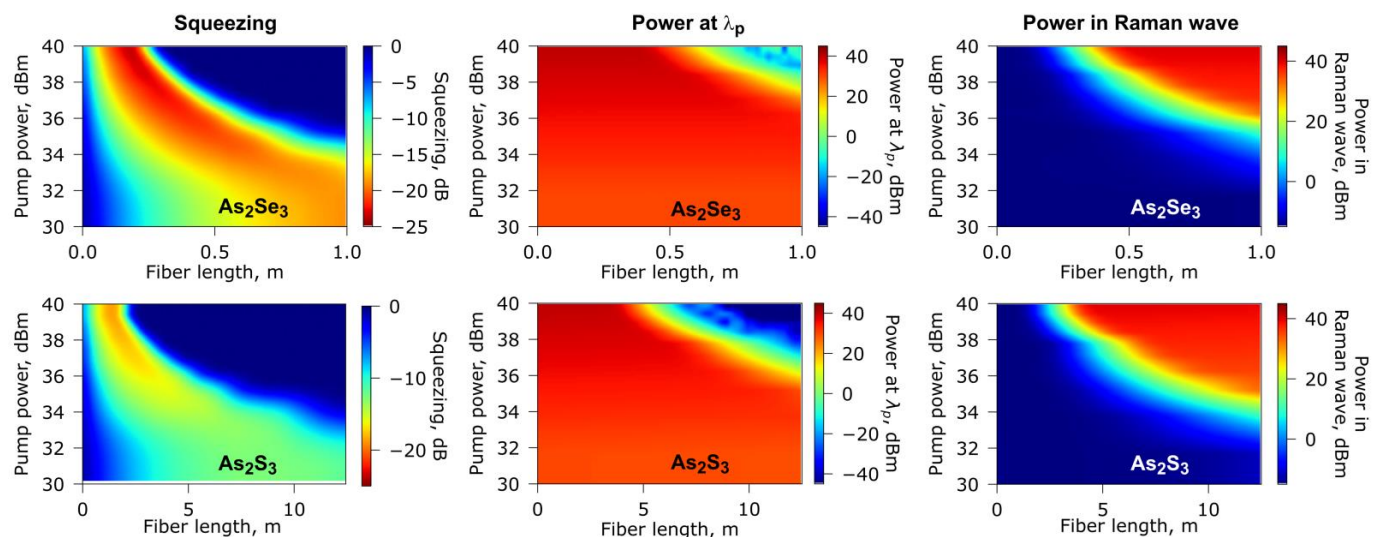
3. Results

We have considered three types of soft glass fibers (As_2Se_3 , As_2S_3 , and tellurite) based on the latest advances in glass technology. Fibers made of As_2Se_3 glass, which have the highest nonlinear refractive index, are successfully fabricated by many scientific groups and commercial companies [33,34,46]. It is known that in the absence of optical losses and inelastic scattering processes, the variance of fluctuations of one quadrature component monotonically decreases with the increasing Kerr parameter $\varphi_{\text{Kerr}} = \gamma P z$ at the initial evolution stage [32]. However, the contribution of parasitic processes deteriorates the noise suppression, and this accumulates as z increases. As such, a fiber design providing large γ values is desirable. We have purposely chosen a small enough diameter of an As_2Se_3 fiber to provide a hugely effective nonlinear Kerr coefficient and single-mode light propagation at a wavelength of $2 \mu\text{m}$. However, further reduction of the diameter may be impractical because it is difficult from a technological point of view and may eventually even be counter-productive from a fundamental point of view because when decreasing the core diameters approaching the sub-wavelength regime, the mode diameter no longer follows the core diameter. When considering an As_2S_3 glass fiber, we specifically selected a commercially available fiber [46] in order to demonstrate that the technical implementation of quantum noise squeezing effects in the proposed approach can be straight-forward. When considering a tellurite fiber, we focused on special fibers that have been reported in the literature [33,41]. We have also analyzed a standard SMF28e silica telecom fiber for comparison. Table 1 summarizes the preset and calculated parameters of the considered fibers.

Table 1. Parameters used in simulations of quantum noise squeezing.

Parameter	Symbol	Dimension	Type of Glass Fiber			
			As ₂ Se ₃	As ₂ S ₃	Tellurite	Silica
Core diameter	d	μm	2.6	5	2.7	8.2
Numerical aperture	NA		0.58	0.3	0.5	0.14
Nonlinear Kerr coefficient	γ	(W km) ⁻¹	5000	400	200	0.6
Dispersion coefficient	β_2	ps ² /km	790	350	170	-80
Fraction of the Raman contribution	f_R		0.1	0.1	0.51	0.2
Optical loss	α	dB/km	60	50	20	20
Pump wavelength	λ_p	μm			2	
Temperature	T	K			300	

Figure 3 shows the results of numerical simulations in the framework of Equations (7)–(14) and taking into account the parameters listed in Table 1. Each row corresponds to a certain type of fiber. Quantum noise squeezing as a function of fiber length and pump power is demonstrated in the left column. As expected, the higher the pump power, the stronger the squeezing. However, the squeezing is not a monotonic function of the fiber length. There are optimal lengths for which the noise suppression is strongest. However, the minimum is broad, and the squeezing near the optimal values is achieved in a fairly wide range of fiber lengths at a fixed light power. Additionally, the higher the power, the shorter the optimal fiber length. To explain these peculiarities, we calculated the power corresponding to the wave at λ_p at the output of the fiber and the power in the Raman wave as functions of fiber length and the pump power (middle and right column, respectively). It is seen that for relatively high pump powers (>36 dBm) and lengths longer than the optimal ones, the deterministic Raman nonlinearity plays a significant role for soft glass fibers. There is significant energy transfer from the wave at λ_p to the Raman wave (powers at λ_p sharply decrease but powers in Raman waves sharply increase towards the right corner in the corresponding panels for soft glasses in Figure 3). For relatively low pump powers (<33 dBm), the deterministic Raman nonlinearity is not very important; the main limiting factor is optical loss. This was checked by additional numerical simulations in which we successively switched off Raman effects, optical loss, and Raman noise and compared the results with the results obtained in the full model. For standard silica fibers, the losses are the main limiting factor for all of the considered power values.

**Figure 3.** *Cont.*

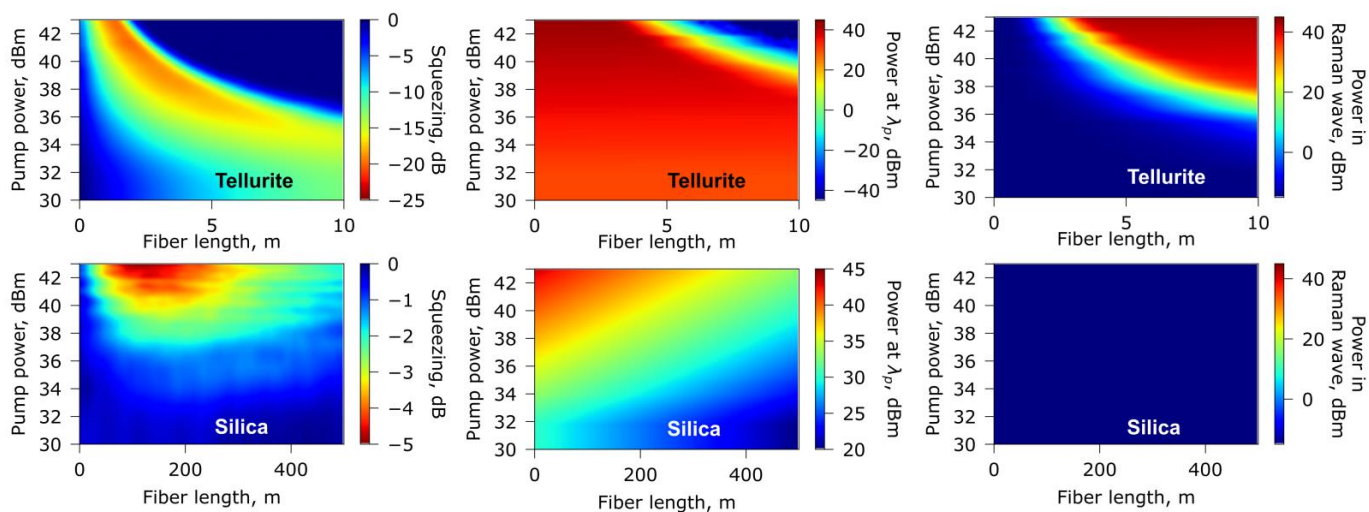


Figure 3. Numerically simulated quantum noise squeezing (left columns), power at the pump wavelength (middle column), and power in Raman wave (right column) as a function of both fiber length and pump power for fibers made of different glasses.

Figure 3 demonstrates that quantum noise squeezing stronger than -20 dB is expected theoretically for customized As_2Se_3 fibers at a propagation distance shorter than 1 m. For As_2S_3 and tellurite glass fibers, the expected squeezing in the -20 – -15 dB range can be reached for fiber lengths of the order of 1 m. Silica fibers are not suitable for strong noise suppression at the wavelength of $2\ \mu\text{m}$ since their losses dramatically deteriorate the squeezed state for the required lengths, which are longer than 100 m.

4. Discussion

In the presented work, we have proposed the generation of multiphoton states of 10-W class light in the 2-micron wavelength range with squeezed quantum fluctuations stronger than -15 dB in chalcogenide and tellurite soft glass fibers with large Kerr nonlinearities. Using a realistic step-index customized design and commercial fibers with nonlinear Kerr coefficients that are 2–4 orders of magnitude larger compared to standard silica fibers, we have numerically studied the possibility of quantum noise squeezing in the framework of the stochastic nonlinear Raman-modified Schrödinger equation by taking into account Kerr nonlinearity, distributed losses, and inelastic light scattering processes. We have theoretically revealed the factors limiting noise suppression. At relatively high pump powers (>36 dBm) and lengths longer than optimal ones, the deterministic Raman nonlinearity plays a significant role in soft glass fibers. For relatively low pump powers (<33 dBm), the deterministic Raman nonlinearity is not very important; the main limiting factor is optical loss. Quantum noise squeezing stronger than -20 dB is numerically predicted for a customized As_2Se_3 fiber for optimal fiber lengths shorter than 1 m. For commercial As_2S_3 and customized tellurite glass fibers, a squeezing in the -20 – -15 dB range can be expected to be reached for fiber lengths of the order of 1 m. We verified that silica fibers are not suitable for strong noise suppression at the $2\ \mu\text{m}$ wavelength since the high optical losses in this regime dramatically deteriorate the nonclassical multiphoton states. As such, our study paves the way for novel fiber sources of nonclassical squeezed light in the 2-micron wavelength that are desirable for numerous applications.

Author Contributions: Conceptualization, G.L., E.A.A. and A.V.A.; methodology, A.A.S., J.F.C. and E.A.A.; software, A.A.S., N.A.K. and E.A.A.; validation, G.L., J.F.C. and A.V.A.; formal analysis, A.A.S., N.A.K. and E.A.A.; investigation, A.A.S., G.L., J.F.C., E.A.A. and A.V.A.; data curation, A.A.S. and E.A.A.; writing—original draft preparation, E.A.A.; writing—review and editing, A.A.S., G.L., J.F.C. and A.V.A. All authors have read and agreed to the published version of the manuscript.

Funding: This research was funded in part by a mega-grant from the Ministry of Science and Higher Education of the Russian Federation, contract no. 075-15-2021-633 (investigating quantum noise squeezing for silica and tellurite fibers), by the Russian Foundation for Basic Research, grant nos. 19-29-11032 (investigating quantum noise squeezing for chalcogenide fibers) and 20-03-00874 (investigating dispersion and nonlinear characteristics of tellurite fibers), and by the Ministry of Science and Higher Education of the Russian Federation, state assignment for the Institute of Applied Physics RAS, project 0030-2021-0012 (investigating dispersion and nonlinear characteristics of chalcogenide and silica fibers). The work by A.A.S. was supported by the Foundation for the Advancement of Theoretical Physics and Mathematics “BASIS”.

Institutional Review Board Statement: Not applicable.

Informed Consent Statement: Not applicable.

Data Availability Statement: Data underlying the results presented in this article may be obtained from the authors upon reasonable request.

Conflicts of Interest: The authors declare no conflict of interest.

References

1. Andersen, U.L.; Gehring, T.; Marquardt, C.; Leuchs, G. 30 years of squeezed light generation. *Phys. Scr.* **2016**, *91*, 053001. [\[CrossRef\]](#)
2. Schnabel, R. Squeezed states of light and their applications in laser interferometers. *Phys. Rep.* **2017**, *684*, 1–51. [\[CrossRef\]](#)
3. Mukamel, S.; Freyberger, M.; Schleich, W.P.; Bellini, M.; Zavatta, A.; Leuchs, G.; Silberhorn, C.; Boyd, R.W.; Sánchez-Soto, L.L.; Stefanov, A.; et al. Roadmap on quantum light spectroscopy. *J. Phys. B At. Mol. Opt. Phys.* **2020**, *53*, 072002. [\[CrossRef\]](#)
4. Appel, J.; Figueira, E.; Korytov, D.; Lobino, M.; Lvovsky, A.I. Quantum Memory for Squeezed Light. *Phys. Rev. Lett.* **2008**, *100*, 093602. [\[CrossRef\]](#)
5. Vahlbruch, H.; Chelkowski, S.; Danzmann, K.; Schnabel, R. Quantum engineering of squeezed states for quantum communication and metrology. *New J. Phys.* **2007**, *9*, 371. [\[CrossRef\]](#)
6. Kaiser, F.; Fedrici, B.; Zavatta, A.; D’Auria, V.; Tanzilli, S. A fully guided-wave squeezing experiment for fiber quantum networks. *Optica* **2016**, *3*, 362–365. [\[CrossRef\]](#)
7. Zhou, L.; Liu, P.; Jin, G.-R. Single-Port Homodyne Detection in a Squeezed-State Interferometry with Optimal Data Processing. *Photonics* **2021**, *8*, 291. [\[CrossRef\]](#)
8. Khalil, E.; Mohamed, A.-B.; Obada, A.-S.; Eleuch, H. Quasi-Probability Husimi-Distribution Information and Squeezing in a Qubit System Interacting with a Two-Mode Parametric Amplifier Cavity. *Mathematics* **2020**, *8*, 1830. [\[CrossRef\]](#)
9. Grote, H.; Danzmann, K.; Dooley, K.L.; Schnabel, R.; Slutsky, J.; Vahlbruch, H. First Long-Term Application of Squeezed States of Light in a Gravitational-Wave Observatory. *Phys. Rev. Lett.* **2013**, *110*, 181101. [\[CrossRef\]](#)
10. Mansell, G.L.; McRae, T.G.; Altin, P.A.; Yap, M.J.; Ward, R.L.; Slagmolen, B.J.J.; Shaddock, D.A.; McClelland, D.E. Observation of Squeezed Light in the 2 μ m Region. *Phys. Rev. Lett.* **2018**, *120*, 203603. [\[CrossRef\]](#)
11. Mehmet, M.; Vahlbruch, H. The Squeezed Light Source for the Advanced Virgo Detector in the Observation Run O3. *Galaxies* **2020**, *8*, 79. [\[CrossRef\]](#)
12. Ralph, T.C.; Lam, P.K. Teleportation with Bright Squeezed Light. *Phys. Rev. Lett.* **1998**, *81*, 5668–5671. [\[CrossRef\]](#)
13. Taylor, M.A.; Janousek, J.; Daria, V.; Knittel, J.; Hage, B.; Bachor, H.; Bowen, W. Biological measurement beyond the quantum limit. *Nat. Photonics* **2013**, *7*, 229–233. [\[CrossRef\]](#)
14. Lassen, M.; Delaubert, V.; Janousek, J.; Wagner, K.; Bachor, H.-A.; Lam, P.K.; Treps, N.; Buchhave, P.; Fabre, C.; Harb, C.C. Tools for Multimode Quantum Information: Modulation, Detection, and Spatial Quantum Correlations. *Phys. Rev. Lett.* **2007**, *98*, 083602. [\[CrossRef\]](#)
15. Heinze, J.; Willke, B.; Vahlbruch, H. Observation of Squeezed States of Light in Higher-Order Hermite-Gaussian Modes with a Quantum Noise Reduction of up to 10 dB. *Phys. Rev. Lett.* **2022**, *128*, 083606. [\[CrossRef\]](#)
16. Yan, M.; Ma, L. Generation of Higher-Order Hermite–Gaussian Modes via Cascaded Phase-Only Spatial Light Modulators. *Mathematics* **2022**, *10*, 1631. [\[CrossRef\]](#)
17. Vahlbruch, H.; Mehmet, M.; Danzmann, K.; Schnabel, R. Detection of 15 dB Squeezed States of Light and their Application for the Absolute Calibration of Photoelectric Quantum Efficiency. *Phys. Rev. Lett.* **2016**, *117*, 110801. [\[CrossRef\]](#)
18. Corney, J.F.; Heersink, J.; Dong, R.; Josse, V.; Drummond, P.D.; Leuchs, G.; Andersen, U.L. Simulations and experiments on polarization squeezing in optical fiber. *Phys. Rev. A* **2008**, *78*, 023831. [\[CrossRef\]](#)
19. McCormick, C.F.; Boyer, V.; Arimondo, E.; Lett, P.D. Strong relative intensity squeezing by four-wave mixing in rubidium vapor. *Opt. Lett.* **2006**, *31*, 178–180. [\[CrossRef\]](#)
20. Shelby, R.M.; Levenson, M.D.; Perlmutter, S.H.; DeVoe, R.G.; Walls, D.F. Broad-Band Parametric Deamplification of Quantum Noise in an Optical Fiber. *Phys. Rev. Lett.* **1986**, *57*, 691–694. [\[CrossRef\]](#)
21. Rosenbluh, M.; Shelby, R.M. Squeezed optical solitons. *Phys. Rev. Lett.* **1991**, *66*, 153–156. [\[CrossRef\]](#) [\[PubMed\]](#)
22. Fiorentino, M.; Sharpen, J.E.; Kumar, P.; Porzio, A.; Windeler, R.S. Soliton squeezing in microstructure fiber. *Opt. Lett.* **2002**, *27*, 649–651. [\[CrossRef\]](#) [\[PubMed\]](#)

23. Fiorentino, M.; Sharping, J.E.; Kumar, P.; Levandovsky, D.; Vasilyev, M. Soliton squeezing in a Mach-Zehnder fiber interferometer. *Phys. Rev. A* **2001**, *64*, 031801. [\[CrossRef\]](#)

24. Tran, T.X.; Cassemiro, K.N.; Söller, C.; Blow, K.J.; Biancalana, F. Hybrid squeezing of solitonic resonant radiation in photonic crystal fibers. *Phys. Rev. A* **2011**, *84*, 013824. [\[CrossRef\]](#)

25. Dong, R.; Heersink, J.; Corney, J.; Drummond, P.; Andersen, U.L.; Leuchs, G. Experimental evidence for Raman-induced limits to efficient squeezing in optical fibers. *Opt. Lett.* **2008**, *33*, 116–118. [\[CrossRef\]](#) [\[PubMed\]](#)

26. Kapasi, D.; Eichholz, J.; McRae, T.; Ward, R.; Slagmolen, B.J.J.; Legge, S.; Hardman, K.S.; Altin, P.; McClelland, D. Tunable narrow-linewidth laser at 2 μ m wavelength for gravitational wave detector research. *Opt. Express* **2020**, *28*, 3280–3288. [\[CrossRef\]](#)

27. Zhang, Q.; Hou, Y.; Wang, X.; Song, W.; Chen, X.; Bin, W.; Li, J.; Zhao, C.; Wang, P. 5 W ultra-low-noise 2 μ m single-frequency fiber laser for next-generation gravitational wave detectors. *Opt. Lett.* **2020**, *45*, 4911–4914. [\[CrossRef\]](#)

28. Zervas, M.N.; Codemard, C.A. High Power Fiber Lasers: A Review. *IEEE J. Sel. Top. Quantum Electron.* **2014**, *20*, 219–241. [\[CrossRef\]](#)

29. Richardson, D.J.; Nilsson, J.; Clarkson, W.A. High power fiber lasers: Current status and future perspectives [Invited]. *J. Opt. Soc. Am. B* **2010**, *27*, B63–B92. [\[CrossRef\]](#)

30. Aleshkina, S.S.; Fedotov, A.; Korobko, D.; Stoliarov, D.; Lipatov, D.S.; Velmiskin, V.; Temyanko, V.L.; Kotov, L.V.; Gumenyuk, R.; Likhachev, M.E. All-fiber polarization-maintaining mode-locked laser operated at 980 nm. *Opt. Lett.* **2020**, *45*, 2275–2278. [\[CrossRef\]](#)

31. Kamynin, V.A.; Wolf, A.A.; Skvortsov, M.I.; Filatova, S.A.; Kopyeva, M.S.; Vlasov, A.A.; Tsvetkov, V.B.; Babin, S.A. Distributed Temperature Monitoring Inside Ytterbium DFB and Holmium Fiber Lasers. *J. Light. Technol.* **2021**, *39*, 5980–5987. [\[CrossRef\]](#)

32. Bachor, H.A.; Ralph, T.C.; Lucia, S.; Ralph, T.C. *A Guide to Experiments in Quantum Optics*; Wiley-vch: Weinheim, Germany, 2004.

33. Tao, G.; Ebendorff-Heidepriem, H.; Stolyarov, A.M.; Danto, S.; Badding, J.V.; Fink, Y.; Ballato, J.; Abouraddy, A.F. Infrared fibers. *Adv. Opt. Photon.* **2015**, *7*, 379–458. [\[CrossRef\]](#)

34. Eggleton, B.J.; Luther-Davies, B.; Richardson, K. Chalcogenide photonics. *Nat. Photon.* **2011**, *5*, 141–148. [\[CrossRef\]](#)

35. Cai, D.; Xie, Y.; Guo, X.; Wang, P.; Tong, L. Chalcogenide Glass Microfibers for Mid-Infrared Optics. *Photonics* **2021**, *8*, 497. [\[CrossRef\]](#)

36. Anashkina, E.A.; Shiryaev, V.S.; Koptev, M.Y.; Stepanov, B.S.; Muravyev, S.V. Development of As-Se tapered suspended-core fibers for ultra-broadband mid-IR wavelength conversion. *J. Non-Cryst. Solids* **2018**, *480*, 43–50. [\[CrossRef\]](#)

37. Anashkina, E.A.; Kim, A.V. Numerical Simulation of Ultrashort Mid-IR Pulse Amplification in Praseodymium-Doped Chalcogenide Fibers. *J. Light. Technol.* **2017**, *35*, 5397–5403. [\[CrossRef\]](#)

38. Kibler, B.; Lemière, A.; Gomes, J.-T.; Gaponov, D.; Lavoute, L.; Désévédavy, F.; Smektala, F. Octave-spanning coherent supercontinuum generation in a step-index tellurite fiber and towards few-cycle pulse compression at 2 μ m. *Opt. Commun.* **2021**, *488*, 126853. [\[CrossRef\]](#)

39. Anashkina, E.A.; Dorofeev, V.V.; Skobelev, S.S.; Balakin, A.A.; Motorin, S.E.; Kosolapov, A.F.; Andrianov, A.V. Microstructured Fibers Based on Tellurite Glass for Nonlinear Conversion of Mid-IR Ultrashort Optical Pulses. *Photonics* **2020**, *7*, 51. [\[CrossRef\]](#)

40. Anashkina, E.A.; Andrianov, A.V. Design and Dispersion Control of Microstructured Multicore Tellurite Glass Fibers with In-Phase and Out-of-Phase Supermodes. *Photonics* **2021**, *8*, 113. [\[CrossRef\]](#)

41. Qin, G.; Liao, M.; Suzuki, T.; Mori, A.; Ohishi, Y. Widely tunable ring-cavity tellurite fiber Raman laser. *Opt. Lett.* **2008**, *33*, 2014–2016. [\[CrossRef\]](#)

42. Snopatin, G.E.; Churbanov, M.F.; Pushkin, A.A.; Gerasimenko, V.V.; Dianov, E.M.; Plotnichenko, V.G. High purity arsenic-sulfide glasses and fibers with minimum attenuation of 12 dB/km. *Optoelectron. Adv. Mater. Rapid Commun.* **2009**, *3*, 669–671.

43. Shiryaev, V.; Churbanov, M.; Snopatin, G.; Chenard, F. Preparation of low-loss core-clad As-Se glass fibers. *Opt. Mater.* **2015**, *48*, 222–225. [\[CrossRef\]](#)

44. Dianov, E.M.; Petrov, M.Y.; Plotnichenko, V.G.; Sysoev, V.K. Estimate of the minimum optical losses in chalcogenide glasses. *Sov. J. Quantum Electron.* **1982**, *12*, 498–499. [\[CrossRef\]](#)

45. Anashkina, E.A.; Andrianov, A.V.; Corney, J.F.; Leuchs, G. Chalcogenide fibers for Kerr squeezing. *Opt. Lett.* **2020**, *45*, 5299–5302. [\[CrossRef\]](#)

46. Available online: <https://irflex.com> (accessed on 12 September 2022).

47. Agrawal, G.P. *Nonlinear Fiber Optics*, 6th ed.; Elsevier: Amsterdam, The Netherlands, 2019.

48. Singh, M.; Singh, A. The Optimal Order Newton’s Like Methods with Dynamics. *Mathematics* **2021**, *9*, 527. [\[CrossRef\]](#)

49. Available online: <http://www.amorphousmaterials.com> (accessed on 12 September 2022).

50. Ghosh, G. Sellmeier Coefficients and Chromatic Dispersions for Some Tellurite Glasses. *J. Am. Ceram. Soc.* **1995**, *78*, 2828–2830. [\[CrossRef\]](#)

51. Drummond, P.; Corney, J. Quantum noise in optical fibers I Stochastic equations. *J. Opt. Soc. Am. B* **2001**, *18*, 139–152. [\[CrossRef\]](#)

52. Corney, J.; Drummond, P. Quantum noise in optical fibers II Raman jitter in soliton communications. *J. Opt. Soc. Am. B* **2001**, *18*, 153–161. [\[CrossRef\]](#)

53. Bonetti, J.; Hernandez, S.; Grosz, D.F. Master equation approach to propagation in nonlinear fibers. *Opt. Lett.* **2021**, *46*, 665–668. [\[CrossRef\]](#)

54. Sorokin, A.A.; Anashkina, E.A.; Corney, J.F.; Bobrovs, V.; Leuchs, G.; Andrianov, A.V. Numerical Simulations on Polarization Quantum Noise Squeezing for Ultrashort Solitons in Optical Fiber with Enlarged Mode Field Area. *Photonics* **2021**, *8*, 226. [\[CrossRef\]](#)

55. Yuan, W. 2–10 μ m mid-infrared supercontinuum generation in As₂Se₃ photonic crystal fiber. *Laser Phys. Lett.* **2013**, *10*, 95107. [\[CrossRef\]](#)

56. Xiong, C.; Magi, E.; Luan, F.; Tuniz, A.; Dekker, S.; Sanghera, J.S.; Shaw, L.B.; Aggarwal, I.D.; Eggleton, B.J. Characterization of picosecond pulse nonlinear propagation in chalcogenide As(2)S(3) fiber. *Appl. Opt.* **2009**, *48*, 5467–5474. [[CrossRef](#)] [[PubMed](#)]
57. Yan, X.; Qin, G.; Liao, M.; Suzuki, T.; Ohishi, Y. Transient Raman response effects on the soliton self-frequency shift in tellurite microstructured optical fiber. *J. Opt. Soc. Am. B* **2011**, *28*, 1831–1836. [[CrossRef](#)]